Design and Synthesis of Novel and Potent Inhibitors of the Type II Transmembrane Serine Protease, Matriptase, Based upon the Sunflower Trypsin Inhibitor-1

Peng Li,[⊥,§] Sheng Jiang,[⊥,#] Sheau-Ling Lee,[†] Cheng Yong Lin,[†] Michael D. Johnson,[†] Robert B. Dickson,[†,‡] Christopher J. Michejda,[#,‡] and Peter P. Roller*[,⊥]

Lombardi Cancer Center, Georgetown University Medical Center, Washington, District of Columbia 20007, Molecular Aspects of Drug Design Section, Structural Biophysics Laboratory, NCI, NIH, Frederick Maryland 21702, and Laboratory of Medicinal Chemistry, NCI, NIH, Frederick, Maryland 21702

Received April 26, 2007

Matriptase, initially isolated from human breast cancer cells in culture, is a member of the emerging class of type II transmembrane serine proteases. Matriptase blockade could potentially modulate tumorigenesis and metastasis *in vivo*. Sunflower trypsin inhibitor-1 (**1**, SFTI-1), isolated from sunflower seeds, exhibits very potent matriptase inhibitory activity. On the basis of these findings, we designed and synthesized 13 analogues of the naturally occurring peptide **1** with the intention to explore the structure−activity relationships of this type of bicyclic peptides and to improve inhibitory selectivity and metabolic stability of the disulfide-bridge-containing peptide **1**. We discovered that the methylenedithioether-bridged compound **14** demonstrates very potent binding affinity to matriptase. Compound **8** exhibits much better selectivity for inhibition of matriptase versus thrombin, whereas compound **2** becomes a more potent thrombin inhibitor, which can be potentially used as an anticoagulant for prophylaxis and therapy of thromboembolism.

Introduction

Protease inhibitors are widely distributed in nature; their main role is to regulate the activities of proteolytic enzymes.[1−2] These inhibitors can be classified into a number of families based on their active-site structures and their specificities to inhibit the cleavage of specific peptide sequences within proteins. Among these, inhibitors of serine proteases are being studied most extensively. Matriptase (MT-SP1, TADG-15, epithin, ST14) is a type II transmembrane serine protease that is found on the surfaces of epithelial cells and certain other cell types.[3−6] Although matriptase is initially synthesized as a transmembrane serine protease, it was isolated originally from cancer cell culture supernatants and from human milk in its activated form, complexed with its cognate Kunitz type serine inhibitor, the hepatocyte growth factor activator inhibitor-1 (HAI-1[a]). Matriptase may function to degrade the extracellular matrix, as well as several cellular regulatory proteins; specifically, it may activate hepatocyte growth factor (HGF) by cleaving its inactive proform, it may activate urokinase by cleaving its zymogen, and it may cleave and activate the protease activated receptor-2 (PAR-2).[7−9] Matriptase is also found as a large transmembrane protein in most cancer cells including human breast cancer cells.[4,5,10] Inhibition of the matriptase enzyme is a logical target for intervention, since it was demonstrated that matriptase can activate key prometastatic substrates, and it may function in epithelial cell migration, cancer invasion, and metastasis.[8] Specifically, matriptase expression, activation, and/or imbalance with HAI-1 has been observed in cancers of the breast, ovary, prostate, kidney, lung, cervix, thyroid gland, colon, and stomach.[11−18] Most recently, matriptase has shown to have robust oncogenic activity for skin carcinogenesis in the transgenic mouse and HAI-1 was potently tumor suppressive.[19−22] Thus, combining the available evidence, it is reasonable to propose that matriptase blockade could have anticancer effects in human.[6,8]

In 2001, our group published the synthesis of the sunflower trypsin inhibitor **1** that was originally isolated from sunflower seeds (Figure 1).[23] Three other groups published their work related to the synthesis of compound **1** around the same time.[24−26] **1** was partially characterized by classical techniques, and its structure was confirmed based on the electron density map of compound **1** cocrystallized with bovine-β-trypsin.[24] **1** is not only the smallest naturally occurring peptidic protease inhibitor isolated to date, with only 14 residues, but it is also the most potent in the Bowman−Birk family of serine protease inhibitors (BBIs). These properties arise from the unique structural features of **1**. This peptide possesses the characteristic 9-mer disulfide-cyclized loop of the BBIs, and its remaining five residues form a second backbone-cyclized ring.[27] To date, over 100 BBIs have been described in the literature.[28] Several papers describing the biological activities of **1** and its analogues were also published.[29−33] Recently, we found that peptide **1** potently inhibits the extracellular matrix serine protease, matriptase, at a nanomolar level.[23] The conformationally constrained structural feature and potent matriptase inhibitory activity of **1** make this inhibitor an attractive template for the

* To whom correspondence should be addressed. Tel: +1 301 846 5904, Fax: +1 301 846 6033, E-mail: proll@helix.nih.gov.
† Georgetown University Medical Center.
# Structural Biophysics Laboratory, NCI.
⊥ Laboratory of Medicinal Chemistry, NCI.
§ Current address: Intracellular Therapies, Inc., New York, New York, 10032.
‡ Deceased.

[a] Abbreviations: BBI, Bowman−Birk inhibitor; Bip, L-4-biphenylalanine; ^{t}Bu, *tert*-butyl DCM, dichloromethane; DIPEA, *N*,*N*′-diisopropylethylamine; FAB-MS, fast atom bombardment mass spectrometry; F_5Phe, L-pentafluorophenylalanine; HAI-1, hepatocyte growth factor activator inhibitor-1; HATU, [dimethylamino-([1,2,3]triazolo[4,5-*b*]pyridin-3-yloxy)methylene]-dimethylammonium hexafluorophosphate; HBTU, [(benzotriazol-1-yloxy)-dimethylaminomethylene]dimethylammonium hexafluorophosphate; HGF, hepatocyte growth factor; HOAt, [1,2,3]triazolo[4,5-*b*]pyridin-3-ol; HOBt, benzotriazol-1-ol; HPLC, high performance liquid chromatography; MALDI-TOF, matrix-assisted laser desorption/ionization time-of-flight; 2-Nal, L-2-naphthylalanine; NMM, *N*-methylmorpholine; PAR-2, protease activated receptor-2; Phe(Gu), 4-(guanidinyl)phenylalanine; Pmc, 2,2,5,7,8-pentamethylchroman-6-sulfonyl; SFTI-1, sunflower trypsin inhibitor-1; SPPS, solid-phase peptide synthesis; TBAF, tetrabutylammonium fluoride; TFA, trifluoroacetic acid; TIS, triisopropylsilane; Trt, triphenylmethyl.

10.1021/jm0704898 CCC: $37.00
Published on Web 11/07/2007

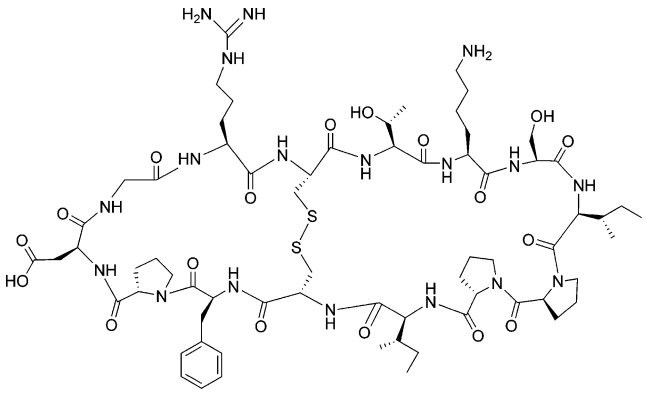

Figure 1. Structure of the bicyclic peptide **1** (SFTI-1).

design of new protease inhibitors with the potential to be used as therapeutic agents for the treatment of cancers.

Results and Discussion

Structure-Based Molecular Design of SFTI-1 Analogues. Compound **1** contains an extensive network of intramolecular hydrogen bonds and also a bisecting disulfide bond, as shown in Figure 2. Such a structural feature makes this bicyclic peptide more rigid which is preferred for high affinity protein binding by virtue of the consequent lowering of the unfavorable entropy loss upon binding. Molecular modeling indicates that the amino acid residues, Arg2, Lys5, Ile10, and Phe12, of compound **1** play important roles in matriptase binding.[23] These residues form various hydrogen bonds and van der Waals interactions with the amino acid residues located in the catalytic site of matriptase. On the basis of this structural information, we designed a series of compound **1** analogues by rationally modifying the side chains of these key amino acid residues of **1** in order to investigate the structure−activity relationships of this type of compounds and to improve their inhibitory selectivity.

Lys5 in **1** plays an important role in protein binding. Its basic side chain is buried deeply inside the binding pocket of matriptase and forms various interactions with the amino acid residues located in the catalytic site of matriptase, as shown in Figure 3. The terminal amino group in Lys5 forms three hydrogen bonds with the backbone and side chain of Ser^{190} as well as the side chain of Asp^{189} of matriptase. On the basis of this structural information, we designed **3** and **6**, in which Lys5 was replaced with L-homo-lysine and L-ornithine, respectively. The adjustment of the side chain length of Lys5 is aimed at optimally positioning the terminal amino group of Lys5 inside the narrow and deep subpocket of matriptase to tune up the interactions between Lys5 and the key amino acid residues of matriptase, such as Asp^{189} and Ser.[190] The same strategy was adopted for the investigation of the key residue Arg2. Thus, **12** was designed by replacing Arg2 with L-homo-arginine. **5** was designed by incorporating citrulline, the urea analogue of arginine, in position 2 (Scheme 1 and Table 1). Phe(Gu)2-containing **4** was designed with the intention to establish additional $\pi-\pi$ interactions between the side-chain phenylene group of Phe(Gu)2 and the adjacent Phe and Trp residues of matriptase. Phe12 of **1** is positioned in a hydrophobic region of matriptase and has $\pi-\pi$ interactions with Phe^{97} and Phe^{99} of matriptase (Figure 3). Therefore, we designed **9**, **10**, and **11** by incorporating more hydrophobic and bulky residues, L-2-naphthylalanine (2-Nal), L-4-biphenylalanine, (Bip) and L-pentafluorophenylalanine (F_5Phe), in position 12 of **1** (Figure 2) to establish more van der Waals and $\pi-\pi$ interactions with the proximal hydrophobic residues of matriptase.

To investigate the importance of the disulfide bridge and conformational requirement of the compound **1** backbone for matriptase binding, we also designed compounds **7** and **13** (Scheme 2). For compound **7**, two cysteines were replaced with two serines to evaluate whether breaking the disulfide bridge will cause a dramatic decrease of matriptase binding affinity or not. For compound **13**, Cys3 was substituted with a homocysteine which results in an extended disulfide bridge.

Metabolic stability of disulfide-containing compounds has always been a major concern during the development and applications of this type of chemicals. During the past decades, great efforts have been made to mimic the disulfide bond with other appropriate linkages to enhance redox stability without losing biological activities and selectivities.[34−38] Considering the structural feature of **1**, which contains an intramolecular disulfide bridge bisecting the macrocycle, we designed a more redox-stable analogue containing a methylenedithioether bridge, compound **14** (Scheme 2). In addition to its better redox stability, this methylenedithioether linker is also reasonably flexible, which allows the macrocycle backbone of compound **14** to adopt a favorable conformation to form an extensive intramolecular hydrogen bond network, as observed in **1**.

Chemistry. To synthesize the disulfide-bridged bicyclic peptides, **2**−**6** and **8**−**12**, we built the suitably protected linear precursors by solid-phase peptide synthesis (SPPS) using Fmoc chemistry at first and then constructed the macrocycles by head-to-tail cyclization. The disulfide bridge was established last, as shown in Scheme 1. Positioning Gly at the C-terminus of linear peptide precursors eliminates the possibility of racemization during resin anchoring and subsequent backbone cyclization. In addition, such disconnection locates the two turn-inducing proline residues in the middle of the linear peptide precursors, which facilitates the N- and C-termini approach to each other, making the head-to-tail macrocyclization more robust. These linear peptide precursors, H-Aaa(2)Cys(Trt)Thr(^{t}Bu)Aaa(5) Ser(^{t}Bu)IleProProAaa(10)Cys(Trt)Aaa(12)ProAsp(O^{t}Bu)Gly-O-Rink, were synthesized on polystyrene-based Rink resin. This type of resin is acid labile, its stability toward bases makes it ideal for Fmoc chemistry-based SPPS, and protected peptides can be readily cleaved from the resin with 1% TFA in DCM, with the overall yields ranging from 20% to 40% calculated based upon the Rink resin. The head-to-tail macrocyclization was achieved successfully using HATU as the coupling reagent and HOAt as the accelerator.[39] After side-chain deprotection with the TFA−TIS−H_2O cocktail, the deprotected peptides were oxidized with oxygen to establish the disulfide bridge. The obtained crude products were purified by a semipreparative reversed-phase C^{18}-HPLC. The purity of each bicyclic product is more than 95% determined by an analytical RP-HPLC. All macrocycles were characterized by FAB and MALDI-TOF mass spectrometers.

The syntheses of monocyclic peptide **7**, hCys-containing peptide **13**, and methylenedithioether-bridged peptide **14** were described in Scheme 2. The linear peptide precursors H-Arg(Pmc)Aaa(3)Thr(^{t}Bu)Lys(Boc)Ser(^{t}Bu)IleProProIleAaa(11)PheProAsp(O^{t}Bu)Gly-O-Rink were synthesized on Rink resin by Fmoc SPPS. After the peptides were cleaved from resin, the obtained linear peptides were cyclized using HATU/HOAt/DIPEA and then deprotected with the TFA−TIS−H_2O cocktail. For compound **13**, the disulfide bridge was constructed by oxidation using the same procedure as described in Scheme 1. For compound **14**, the methylenedithioether bridge was established by treating intermediate **21** with tetrabutylammonium fluoride (TBAF).[35−37]

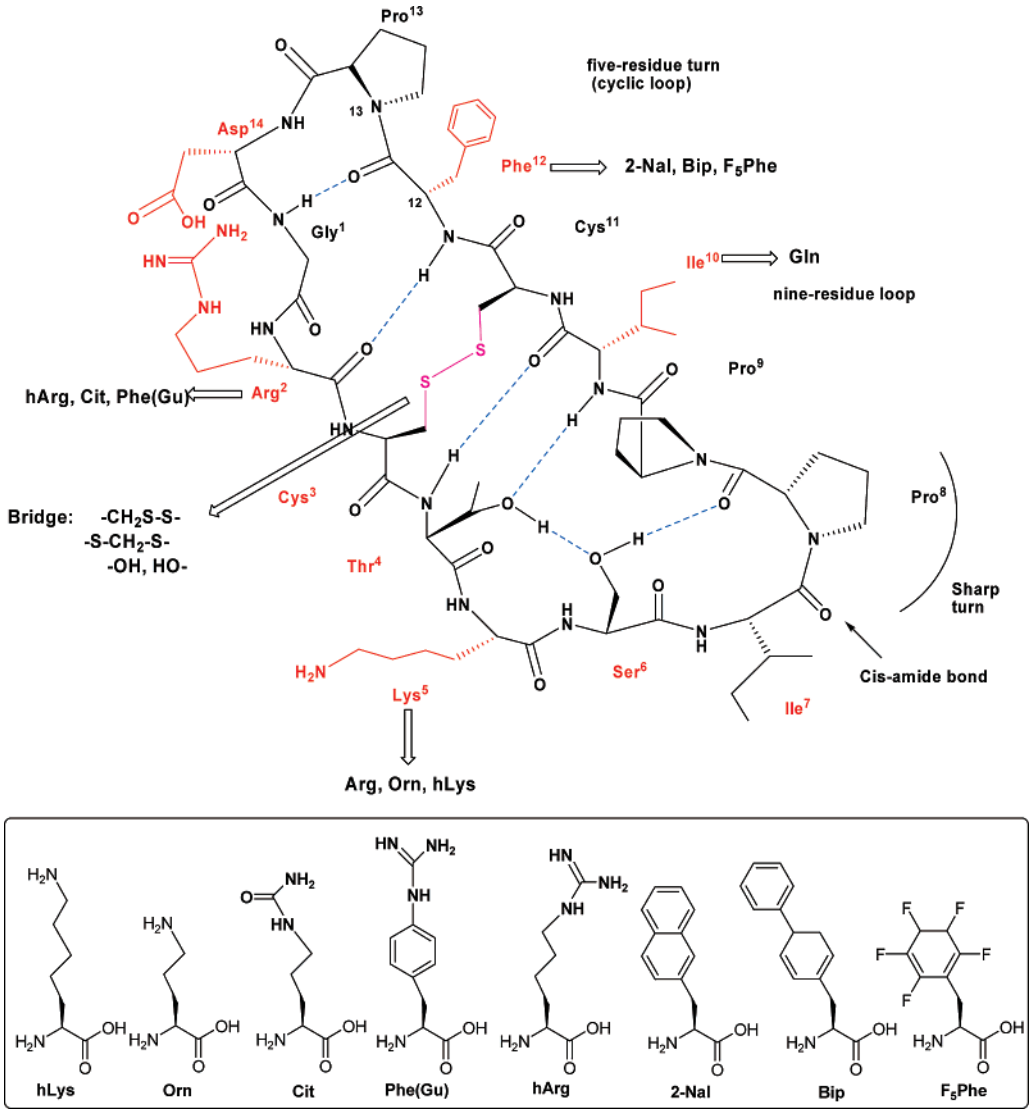

Figure 2. Intramolecular hydrogen bond network of **1**. The amino acid residues colored in red were found to have interactions with matriptase. Structures of incorporated unnatural amino acids were shown at the bottom.

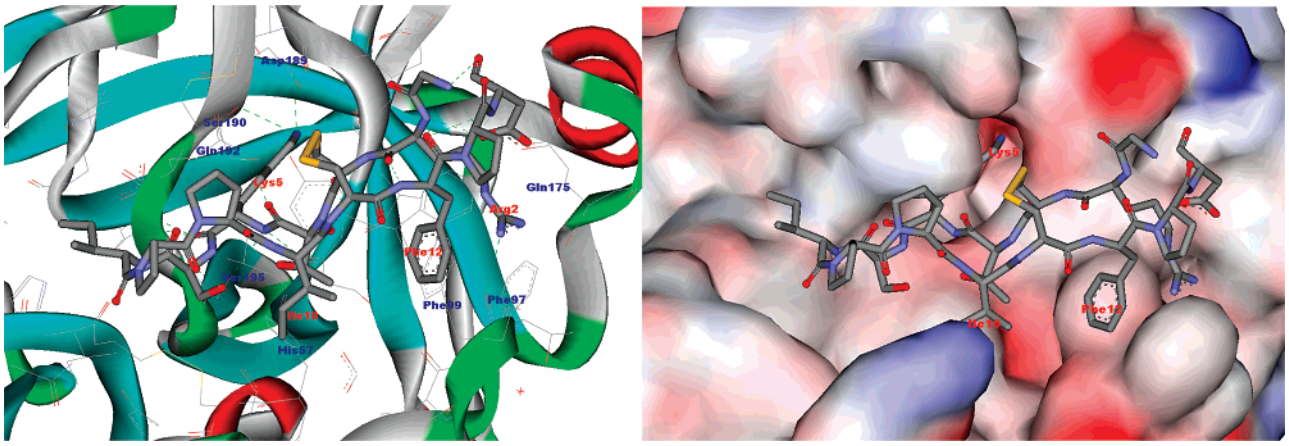

Figure 3. The active site of matriptase complexed with the bicyclic peptide **1**. (A) Protein matriptase is presented as a solid ribbon diagram. Inhibitor **1** is shown in stick style. Hydrogen bonds are presented as green dotted lines. Key amino acid residues that have multiple interactions with **1** are labeled in blue. (B) Surface presentation of the active site of matriptase. The Lys5 side chain of inhibitor **1** is buried deeply in the specificity pocket of matriptase.

Biological Results

As shown in Figure **3**, the basic side chain of Lys5 forms key hydrogen bonds with the amino acid residues located in the catalytic site of matriptase. Asp[189] and Ser[190] in the specificity pocket of matriptase can accept basic amino acids, such as lysine and arginine. Interestingly, replacing Lys5 with a guanidyl-containing arginine significantly changed the selectivity of the resulting compound **2**. Compound **2** actually

Scheme 1. General Procedure for the Synthesis of the Bicyclic Peptides **2**−**6** and **8**−**12**[a]

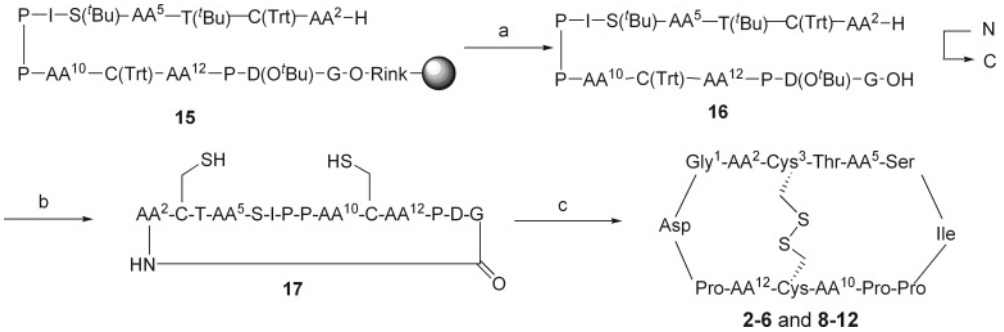

[a] Reagents and conditions: (a) 1% TFA in DCM, 2 min, 20 times; (b) (1) HATU/HOAt/DIPEA in DCM; (2) 95% TFA, 2.5% TIS and 2.5% H_2O, 2 h; (c) O_2, H_2O, overnight.

Table 1. Matriptase and Thrombin Inhibitory Activity of the Cyclic Peptides **1**−**14**[a]

	compound description						
compd	AA^2	AA^5	AA^{10}	AA^{12}	matriptase inhibitory activity [K_i (μM)][b]	thrombin inhibitory activity [K_i (μM)][b]	selectivity
1	Arg	Lys	Ile	Phe	0.1	5	50
2	Arg	Arg	Ile	Phe	4.75	0.86	0.18
3	Arg	Orn	Ile	Phe	>250	inactive	−
4	Phe(Gu)	Lys	Ile	Phe	90	163.6	1.8
5	Cit	Lys	Ile	Phe	22.5	826.8	37
6	Arg	hLys	Ile	Phe	28	45.6	1.6
7	$Ser^{3,7}$, monocyclic peptide				107	40.4	0.38
8	Arg	Lys	Gln	Phe	2.33	>2500	>1073
9	Arg	Lys	Ile	2-NaI	0.45	16.3	36
10	Arg	Lys	Ile	Bip	1.0	25.6	25.6
11	Arg	Lys	Ile	**F_5Phe**	0.89	33.6	37.8
12	hArg	Lys	Ile	Phe	0.857	7.63	8.9
13	$hCys^3$, Cys^{11}				0.38	n.d.[c]	−
14	methylene dithioether bridge				0.16	10	62.5

[a] The binding assay was performed on a Hitachi F4500 instrument using the method described in the Experimental Section. [b] The K_i values were determined by Dixon plots from two sets of data with different concentrations of substrate. [c] n.d. = not determined.

Scheme 2. Synthesis of the Cyclic Peptides **7**, **13**, and **14**[a]

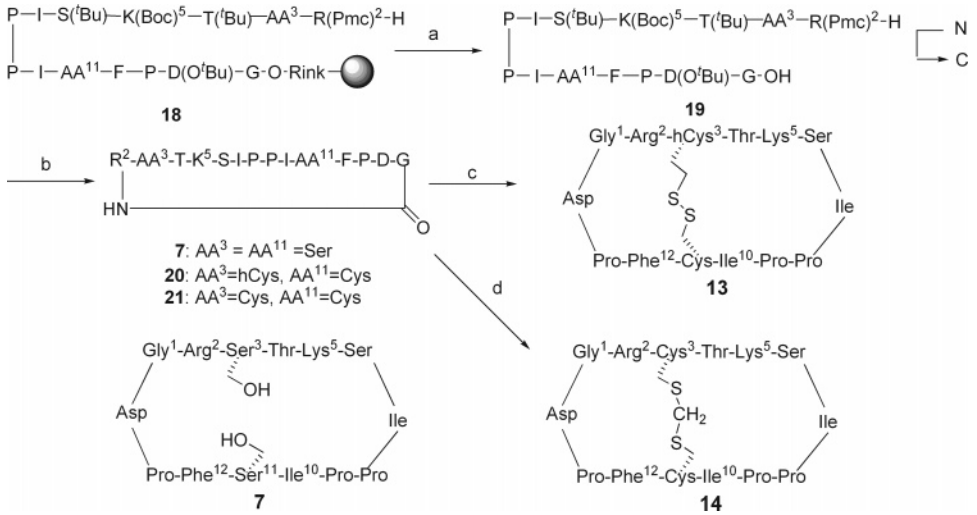

[a] Reagents and conditions: (a) 1% TFA in DCM, 2 min, 20 times; (b) (1) HATU/HOAt/DIPEA in DCM; (2) 95% TFA, 2.5% TIS and 2.5% H_2O, 2 h; (c) O_2, H_2O, overnight; (d) TBAF, DCM/CH_3CN (1:1), 20 min.

becomes a more potent inhibitor of thrombin as shown in Table 1. Although the reverse of inhibitory selectivity of **2** is unexpected, this Arg5-containing compound can be possibly used as an anticoagulant for prophylaxis and therapy of thromboembolism.[40] On the basis of the superimposition of the published crystal structures of human matriptase and thrombin and the sequence alignment of both proteins, we found out that Ser^{190} and Gln^{192} in the specificity pocket of matriptase were replaced with Ala^{190} and Glu^{192} in thrombin. For compound **2**, the positive charged guanidyl-containing side chain of Arg5 is preferred to form salt bridges with the acidic side chain of Glu^{192} in thrombin than with the side chain of Gln^{192} in matriptase. Orn5-containing **3** is remarkably weaker than the parent compound **1**, which indicates that the shortening of the Lys5 side chain disrupted the crucial hydrogen bonds formed between Lys5 and the key residues, Asp^{189} and Ser^{190}, of matriptase, as shown in Figure 3A. Matriptase inhibitory activity decreased 280-fold if the side chain of Lys5 was lengthened by one carbon

(**6** vs **1**). This dramatic activity and selectivity change reflect the importance of Lys5 on selective matriptase binding and also indicate that the naturally occurring lysine is the optimal residue in position 5 of compound **1**.

After determining the optimal side-chain length of the key residue Lys5, we investigated another important residue of compound **1**, Arg2. This residue forms a hydrogen bond with the carbonyl group of Phe^{97} in matriptase, and it also has van der Waals interactions with Trp^{215}, as shown in Figure 3A. The Phe(Gu)2-containing inhibitor **4** was designed and synthesized to try to establish additional $\pi-\pi$ interactions between the phenylene group of the Phe(Gu) and the indolyl group of Trp^{215} of matriptase. However, the inhibitory activity of compound **4** is 900-fold weaker than that of the lead compound **1** (Table 1). The side chain of Phe(Gu) is less flexible than arginine, which may not allow the terminal guanidyl group to form a hydrogen bond with Phe^{97} of matriptase. The disruption of the hydrogen bond is likely to be the major cause of the binding affinity drop of compound **4**. The importance of the hydrogen bond can also be justified by comparing the matriptase inhibitory activity of Cit2-containing **5** with that of **1**. Compound **5** exhibits a much weaker inhibitory activity than **1**, which should be attributed to the replacing the guanidinium functional group of Arg2 with a neutral urea moiety. If the side chain of Arg2 was lengthened by one carbon atom, the resulting hArg2-containing **12** also showed weaker matriptase inhibitory activity than **1**. On the basis of these remarkable changes of matriptase inhibitory activity caused by the minor modifications of the Arg2 side chain, we can conclude that the guanidinium functional group of Arg2 plays an important role for these compounds to bind to matriptase.

Phe12 of **1** is located in a hydrophobic region of matriptase, and it has $\pi-\pi$ and van der Waals interactions with Phe97 and Phe99 of matriptase, as shown in Figure **3**. Therefore, introducing a more hydrophobic amino acid into position 12 of **1** is likely to further improve these hydrophobic interactions. The commercially available unnatural amino acids, 2-Nal, Bip, and F_5Phe, were selected to replace Phe12 since their larger hydrophobic surface areas and π planes may establish additional or stronger interactions with the phenylanilines in the hydrophobic region of matriptase. As shown in Table 1, the matriptase inhibitory activity of the 2-Nal-containing compound **9**, Bip-containing **10**, and F_5Phe-containing **11** are 4.5, 10, and 8.9 times less potent than that of **1**, respectively. Molecular modeling indicates that the phenyl ring of Phe12 cannot form preferred parallel stacking with the phenyl rings of Phe^{97} and Phe^{99} of matriptase. This may explain the insignificant change of the matriptase binding affinities of these analogues. In addition, Phe12 is partially exposed to solvent, and so the entropic penalty for solvating more bulky and hydrophobic residues, such as 2-Nal and Bip, may be another cause for the slight decrease of matriptase binding affinity.

Ile10 of compound **1** is located in a cavity in the proximity of the characteristic insertion loop of matriptase, and it mainly interacts with His^{57} of matriptase, as shown in Figure 3. For matriptase, the amino acid sequence composing the lid region is HCYIDDRGFRYSD, which is quite different from the sequence of thrombin in this region, HCLLYPPWDKNFT. In addition, the insertion loop of matriptase is rotated away from the catalytic site creating a more open cavity than in thrombin. Therefore, a more bulky residue can be accommodated in this cavity for matriptase, whereas a small and hydrophobic residue is preferred in this region for thrombin due to the blockage of the YPPW motif. For example, compound **8**, developed by replacing the Ile10 with a more polar and bulky amino acid residue Gln, demonstrates much weaker thrombin inhibitory activity and better selectivity than the lead compound **1**. The inhibitory selectivity of **8** toward matriptase *versus* thrombin is more than 1073-fold, as shown in Table 1. These findings provide an encouraging starting point for the further development of more selective and potent matriptase inhibitors by modifying the amino acid residue in position 10 of these bicyclic peptides.

On the basis of the fact that a disulfide bond generally is not redox stable, we investigated the functional significance of the disulfide bridge in **1** and tried to replace it with a more stable linkage without losing compound biological activities. At first, we designed and synthesized **7** by replacing of Cys3 and Cys11 with two serines. The matriptase inhibitory potency of the monocyclic **7** decreased 1070-fold, as shown in Table **1**. Compound **7** actually becomes a relatively more potent inhibitor of thrombin. It is very likely that the disruption of the disulfide bridge causes overall conformational change of **7** and consequently leads to the dramatic change of compound biological activities. The disulfide bridge of compound **13** is one carbon atom longer than that of **1**. Such a variation did not cause a significant decrease of matriptase inhibitory activity (Table 1). This indicates that the disulfide bridge can tolerate some minor changes, and it also encourages us to insert a methylene group into the disulfide bridge to develop a methylenedithioether-bridged analogue. The methylenedithioether bridge of **14** has almost the same length with the dithiomethyl bridge of **13** formed between the side chains of homoCys3 and Cys11, and both bridges have similar dihedral angles and flexibility. Compound **14** exhibits similar matriptase inhibitory potency and selectivity with **1**. In addition, the incorporated methylenedithioether linker has been documented to be more stable than the redox-labile disulfide linker.[41] On the basis of the SAR studies described above, we already know that the breaking of the disulfide bridge in **1** will cause significant loss of matriptase inhibitory activity. Therefore, compound **14** should be more promising as a drug candidate.

Conclusion

Matriptase is a transmembrane bound serine protease. It promotes cancer onset and cancer cell metastasis through its proteolytic function. Natural product **1** is a unique bicyclic peptide that potently inhibits matriptase at nanomolar concentrations. On the basis of this lead compound, we designed and synthesized 13 analogues to study the structure−activity relationships of this type of compounds and develop more promising drug candidates. We found that Arg2 and Lys5 are two crucial amino acid residues in **1**, and minor to moderate modifications will cause dramatic changes of matriptase inhibitory activity and selectivity. For instance, **2** becomes a more potent inhibitor of thrombin, which can be potentially used as an anticoagulant for prophylaxis and therapy of thromboembolism. Ile10 is located in a cavity in the proximity of the characteristic loop of matriptase, which provides an opportunity to fine-tune matriptase inhibitory selectivity of these bicyclic compounds by the modification of Ile10. This can be illustrated by the 20-fold enhancement of the matriptase inhibitory selectivity of compound **8**, which was obtained by replacing the hydrophobic Ile10 with a relatively more hydrophilic and bulky Gln10. The intramolecular disulfide bridge in **1** was found to be very important for selective matriptase binding. The methylenedithioether-bridged **14** was discovered as a more redox-stable and potent matriptase inhibitor, which can be served

as a promising lead for the development of therapeutic agents targeting matriptase. Considering the structural complexity and unique biological properties of these bicyclic compounds, the structure−activity information collected in this work may be useful for rationally developing the second generation of matriptase inhibitors in this series.

Experimental Section

General Procedure for the Preparation of the Cyclic Peptides: Synthesis of the Linear Peptide Precursors. Each linear peptide precursor was synthesized with an ABI 433A Peptide Synthesizer, starting with Fmoc-Gly-Rink resin (0.1 mmol) for establishing the C-terminal carboxy functionality, and using the chemical protocols based on Fmoc chemistry (coupling with HBTU/HOBt/DIPEA in NMP). After the completion of the peptide chain elongation, the peptide-bound resin was washed with DMF (3 × 3 mL), DCM (3 × 3 mL), and MeOH (3 × 3 mL), successively. The peptide-bound resin was preswollen with DCM in a sealable sintered glass funnel for 10 min and then the excess DCM was removed. To this reaction funnel was added 1% TFA/DCM (10 mL) and shaken for 2 min. The solution was collected by filtration and neutralized with 10% NMM/MeOH in an ice bath. This cleavage procedure was repeated 10 times, and then the resin was washed with DCM (3 × 30 mL), MeOH (3 × 30 mL), DCM (2 × 30 mL), and MeOH (3 × 30) successively. The combined filtrate was evaporated to dryness in vacuo. The obtained crude peptide, **16** or **19**, was used in the next step without further purification.

Backbone Macrocyclization. The crude side chain-protected peptide (0.1 mmol) was dissolved in anhydrous DCM (250 mL) under nitrogen. The solution was cooled with an ice bath, and then DIPEA (0.6 mmol), HATU (0.3 mmol), and HOAt (0.3 mmol) were added. The reaction mixture was vigorously stirred at ambient temperature for 36 h. The reaction mixture was quenched and acidified with 30% AcOH and then concentrated into thick oil under high vacuum. The obtained intermediate was used as such in the step.

Side Chain Deprotection. The crude protected cyclic peptide was treated with 95% TFA containing 2.5% each of triisopropylsilane (TIS) and water at room temperature for 2 h, and then the solvent was removed under reduced pressure to give backbone cyclized peptide, **17**, **20**, or **21**. For the monocyclic compound **7**, this is the final step. The obtained crude product was purified by a semipreparative HPLC to give the final product **7**.

Disulfide Bridge Formation. The crude deprotected cyclic peptide, **17**, **20**, or **21**, was dissolved in 250 mL of deionized water, which was adjusted to pH 8.5 with ammonium acetate and ammonium hydroxide. The reaction mixture was bubbled with oxygen for 6 h and then stirred at room temperature overnight. The reaction mixture was acidified by adding 30% AcOH, and the resulting solution was lyophilized to give crude product.

Peptide Purification and Characterization. Crude products were purified on three different types of semipreparative columns using different HPLC methods. Method I: Vydac C4 column (22 × 250 mm); solvent system, A, 0.05% TFA in water; B, 0.05% TFA in 90% acetonitrile in water; gradient, 10% to 80% B over 30 min; flow rate, 10.0 mL/min; wavelength, 225 nm. Method II: Vydac C18 column (22 × 250 mm); gradient, 0% to 50% B over 30 min; flow rate, 15.0 mL/min; wavelength, 225 nm. Method III: Vydac C8 column (22 × 250 mm); gradient, 10% to 80% B over 30 min; flow rate, 10.0 mL/min; wavelength, 225 nm. The purity of products was determined by two different types of analytical reversed-phase columns using different HPLC methods. Method A: Merck Chromolith Performance RP-18e column (100 × 4.6 mm); gradient 10% to 50% B over 9 min; flow rate, 5.0 mL/min; wavelength, 225 nm. Method B: Agilent Zorbax 3.5 μm SB−CN column (75 × 4.6 mm); gradient 10% to 60% B over 12 min; flow rate, 2.0 mL/min; wavelength, 225 nm. Purified products were further characterized by Kompact Axima-CFR MALDI-TOF and/or VG Analytical 7070E-HF FAB mass spectrometers.

2. Compound was synthesized according to the general synthetic procedure described in the above. Crude product was purified on a semipreparative column using the HPLC method I (t_R = 18.0 min). The purity of the product was analyzed using the HPLC method A (t_R = 5.13 min, purity 97%) and method B (t_R = 6.62 min, purity 96%). FAB-MS ($M + H^+$): 1542.8.

3. Crude product was purified using the semipreparative HPLC method I (t_R = 17.5 min). The purity of the product was determined using the analytical HPLC method A (t_R = 4.88 min, purity 98%) and method B (t_R = 6.43 min, purity 98%). FAB-MS ($M + H^+$): 1500.8.

4. Crude product was purified using the semipreparative HPLC method I (t_R = 18.2 min). The purity of the product was determined using the analytical HPLC method A (t_R = 5.25 min, purity 98%) and method B (t_R = 6.63 min, purity 98%). FAB-MS ($M + H^+$): 1562.8.

5. Crude product was purified using the semipreparative HPLC method I (t_R = 18.9 min). The purity of the product was determined using the analytical HPLC method A (t_R = 5.71 min, purity 99%) and method B (t_R = 6.78 min, purity 99%). FAB-MS ($M + H^+$): 1515.8.

6. Crude product was purified using the semipreparative HPLC method I (t_R = 17.9 min). The purity of the product was determined using the analytical HPLC method A (t_R = 5.33 min, purity 97%) and method B (t_R = 6.48 min, purity 96%). FAB-MS ($M + H^+$): 1528.8.

7. Crude product was purified using the semipreparative HPLC method I (t_R = 16.0 min). The purity of the product was determined using the analytical HPLC method A (t_R = 4.49 min, purity 95%) and method B (t_R = 5.67 min, purity 95%). FAB-MS ($M + H^+$): 1484.7.

8. Crude product was purified using the semipreparative HPLC method I (t_R = 15.1 min). The purity of the product was determined using the analytical HPLC method A (t_R = 3.44 min, purity 96%) and method B (t_R = 5.00 min, purity 97%). FAB-MS ($M + H^+$): 1529.8.

9. Crude product was purified using the semipreparative HPLC method II (t_R = 19.8 min). The purity of the product was determined using the analytical HPLC method A (t_R = 5.79 min, purity 99%) and method B (t_R = 6.92 min, purity 99%). FAB-MS ($M + H^+$): 1564.8.

10. Crude product was purified using the semipreparative HPLC method III (t_R = 22.0 min). The purity of the product was determined using the analytical HPLC method A (t_R = 6.27 min, purity 99%) and method B (t_R = 7.33 min, purity 98%). FAB-MS ($M + H^+$): 1590.9.

11. Crude product was purified using the semipreparative HPLC method I (t_R = 19.4 min). The purity of the product was determined using the analytical HPLC method A (t_R = 5.61 min, purity 99%) and method B (t_R = 7.00 min, purity 99%). FAB-MS ($M + H^+$): 1604.7.

12. Crude product was purified using the semipreparative HPLC method I (t_R = 18.2 min). The purity of the product was determined using the analytical HPLC method A (t_R = 4.81 min, purity 98%) and method B (t_R = 6.51 min, purity 98%). FAB-MS ($M + H^+$): 1528.8.

13. Crude product was purified using the semipreparative HPLC method I (t_R = 19.0 min). The purity of the product was determined using the analytical HPLC method A (t_R = 4.94 min, purity 95%) and method B (t_R = 6. 39 min, purity 95%). FAB-MS ($M + H^+$): 1527.7.

14. The crude monocyclic peptide **21** (21.6 mg, 0.0142 mmol) was suspended in helium-purged CH_2Cl_2/CH_3CN (30 mL, 1:1), and then TBAF (93 mg, 0.355 mmol) was added into the suspension. The reaction mixture was stirred at room temperature for 20 min and then quenched with glacial acetic acid (100 μL). Solvent was removed under reduced pressure, and the remaining residue was purified using the semipreparative HPLC method III (t_R = 17.5 min). The purity of the product was determined using the analytical HPLC method A (t_R = 5.00 min, purity 95%) and method B (t_R = 6.17 min, purity 96%). MALDI-TOF−MS ($M + H^+$): 1527.7.

Determination of Inhibitory Activity. The 70-kDa activated matriptase was isolated as described previously.[5,10] Bovine thrombin, Bowman−Birk inhibitor (BBI), and the fluorescent substrates were purchased from Sigma (Sigma Chemical Co., St. Louis, MO). Inhibitory activity of **1**−**14** to proteases was measured at room temperature in two different systems. In the first assay system, a reaction buffer of 100 mM Tris-HCl (pH 8.5) containing 100 mg/mL of bovine serum albumin was used. To a cuvette containing 170 μL of reaction buffer were added 10 μL of enzyme solution and 10 μL of inhibitor solution. After preincubation, a solution of the fluorescent peptide substrate (10 μL) was added and the cuvette content was mixed thoroughly. The residual enzyme activity was determined by following the change of fluorescence released by the hydrolysis of the substrates, using a fluorescent spectrophotometer (Hitachi F4500) with excitation wavelength of 360 nm and emission at 480 nm. Fluorescent peptide t-Boc-Gln-Ala-Arg-AMC was used as substrate for matriptase. Peptide N-t-Boc-Leu-Arg−Arg-AMC was used as substrate for thrombin. Hydrolysis rates were recorded in presence of six to seven different concentrations of inhibitor **1** or its analogues. The K_i values were determined by Dixon plots from two sets of data with different concentrations of substrate. The second assay system produced essentially identical results and made use of a t-Boc-Gln-Ala-Arg-AFC peptide as the substrate for matriptase in a buffer of 100 mM Tris (pH 8.3) containing 100 mg/mL of BSA. Assays were conducted with purified matriptase in a total volume of 200 μL in black wall 96-well plates using a Tecan Ultra fluorometer (Tecan, Durham, NC).

Acknowledgment. This research was supported by the Intramural Research Program of the NIH, National Cancer Institute, Frederick, Maryland. R.B.D., S.L.L., C.Y.L., and M.D.J. were supported by NIH R01 CA096851 and R01 CA 104944-01.

Supporting Information Available: Table of the analytical RP-HPLC and MS data of the cyclic peptides **2**−**14**, sequence alignment of matriptase and thrombin, and molecular modeling details. This material is available free of charge via the Internet at http://pubs.acs.org.

References

(1) Laskowski, M.; Kato, I. Protein inhibitors of proteinases. *Annu. Rev. Biochem*. **1980**, *49*, 593−626.
(2) Laskowski, M.; Qasim, M. A. What can the structures of enzyme-inhibitor complexes tell us about the structures of enzyme substrate complexes? *Biochim. Biophys. Acta*. **2000**, *1477*, 324−337.
(3) List, K.; Bugge, T. H.; Szabo, R. Matriptase: potent proteolysis on the cell surface. *Mol. Med.* **2006**, *12*, 1−7.
(4) (a) Lin, C.-Y.; Wang, J.-K.; Torri, J.; Dou, L.; Sang, Q. X. A.; Dickson, R. B. Characterization of a novel, membrane-bound, 80-kDa matrix-degrading protease from human breast cancer cells. Monoclonal antibody production, isolation, and localization. *J. Biol. Chem.* **1997**, *272*, 9147−9152. (b) Oberst, M. D.; Singh, B.; Ozdemirli, M.; Dickson, R. B.; Johnson, M. D.; Lin, C. Y. Characterization of matriptase expression in normal human tissues. *J. Histochem. Cytochem.* **2003**, *51*, 1017−1025.
(5) Lin, C.-Y.; Anders, J.; Johnson, M.; Sang, Q. A.; Dickson, R. B. Molecular cloning of cDNA for matriptase, a matrix-degrading serine protease with trypsin-like activity. *J. Biol. Chem.* **1999**, *274*, 18231−18236.
(6) Hooper, J. D.; Clements, J. A.; Quigley, J. P.; Antalis, T. M. Type II transmembrane serine proteases. Insights into an emerging class of cell surface proteolytic enzymes. *J. Biol. Chem.* **2001**, *276*, 857−860.
(7) Takeuchi, T.; Harris, S.; Hwang, W.; Yan, K. W.; Coughlin, S. R.; Craik, C. S. Cellular localization of membrane-type serine protease 1 and identification of protease-activated receptor-2 and single-chain urokinase-type plasminogen activator as substrates. *J. Biol. Chem.* **2000**, *275*, 26333−26342.
(8) Lee, S.-L.; Dickson, R. B.; Lin, C. Y. Activation of hepatocyte growth factor and urokinase/plasminogen activator by matriptase, an epithelial membrane serine protease. *J. Biol. Chem.* **2000**, *275*, 36720−36725.
(9) Kawaguchi, T.; Qin, L.; Shimomura, T.; Kondo, J.; Matsumoto, K.; Denda, K.; Kitamura, N. Purification and cloning of hepatocyte growth factor activator inhibitor type 2, a Kunitz-type serine protease inhibitor. *J. Biol. Chem.* **1997**, *272*, 27558−27564.
(10) Lin, C.-Y.; Anders, J.; Johnson, M.; Dickson, R. B. Purification and characterization of a complex containing matriptase and a Kunitz-type serine protease inhibitor from human milk. *J. Biol. Chem.* **1999**, *274*, 18237−18242.
(11) (a) Oberst, M.; Anders, J.; Snow, D.; Xie, B.; Singh, B.; Ossandon, M.; Johnson, M. D.; Dickson, R. B.; Lin, C. Y. Matriptase and HAI-1 are expressed by normal and malignant epithelial cells in vitro and in vivo. *Am. J. Pathol*. **2001**, *158*, 1301−1311. (b) Kang, J. Y.; Dolled-Filhard, M.; Ocal, I. T.; Singh, B.; Lin, C. Y.; Dickson, R. B.; Rimm, D. L.; Camp, R. L. Tissue microarray analysis of hepatocyte growth factor/Met pathway components reveals a role for Met, matriptase, and hepatocyte growth factor activator inhibitor 1 in the progression of node-negative breast cancer. *Cancer. Res.* **2003**, *63*, 1101−1105. (c) Oberst, M. D.; Johnson, M. D.; Dickson, R. B.; Lin, C. Y.; Singh, B.; Stewart, M.; Williams, A.; al-Nafussi, A.; Smyth, J. F.; Gobra, H.; Sellar, G. Expression of the serine protease matriptase and its inhibitor HAI-1 in epithelial ovarian cancer: correlation with clinical outcome and tumor clinicopathological parameters. *Clin. Cancer Res.* **2002**, *8*, 1101−1107. (d) Saleem, M.; Adhami, V. M.; Longley, J. B.; Reagan-Shaw, S.; Jarrard, D. F.; Dickson, R. B.; Lin, C. Y.; Mukhtar, H. A novel biomarker for staging human prostate adenocarcinoma: overexpression of matriptase with concomitant loss of its inhibitor, hepatocyte growth factor activator inhibitor-1. *Cancer Epidemiol. Biomarkers Prev.* **2006**, *15*, 217−227.
(12) Galkin, A. V.; Mullen, L.; Fox, W. D.; Brown, J.; Duncan, D.; Moreno, O.; Madison, E. L.; Agus, D. B. CVS-3983, a selective matriptase inhibitor, suppresses the growth of androgen independent prostate tumor xenografts. *Prostate* **2004**, *61*, 228−235.
(13) Jin, J. S.; Chen, A.; Hsieh, D. S.; Yao, C. W.; Cheng, M. F.; Lin, Y. F. Expression of serine protease matriptase in renal cell carcinoma: correlation of tissue microarray immunohistochemical expression analysis results with clinicopathological parameters. *Int. J. Surg. Pathol.* **2006**, *14*, 65−72.
(14) (a) Hoang, C. D.; D'Cunha, J.; Kratzke, M. G.; Casmey, C. E.; Frizelle, S. P.; Maddaus, M. A.; Kratzke, R. A. Gene expression profiling identifies matriptase overexpression in malignant mesothelioma. *Chest* **2004**, *125*, 1843−1852. (b) Lee, J. W.; Yong, S.; Choi, J. J.; Lee, S. J.; Kim, B. G.; Park, C. S.; Lee, J. H.; Lin, C. Y.; Dickson, R. B.; Bae, D. S. Increased expression of matriptase is associated with histopathologic grades of cervical neoplasia. *Hum. Pathol.* **2005**, *36*, 626−633.
(15) Ito, Y.; Akinaga, A.; Yamanaka, K.; Nakagawa, T.; Kondo, A.; Dickson, R. B.; Lin, C. Y.; Miyauchi, A.; Taniguchi, N.; Miyoshi, E. Co-expression of matriptase and N-acetylglucosaminyltransferase V in thyroid cancer tissues-its possible role in prolonged stability in vivo by aberrant glycosylation. *Glycobiology* **2006**, *16*, 368−374.
(16) Zeng, L.; Cao, J.; Zhang, X. Expression of serine protease SNC19/matriptase and its inhibitor hepatocyte growth factor activator inhibitor type 1 in normal and malignant tissues of gastrointestinal tract. *World J. Gastroenterol*. **2005**, *11*, 6202−6207.
(17) Tanimoto, H.; Shigemasa, K.; Tian, X.; Gu, L.; Beard, J. B.; Sawasaki, T.; O'Brien, T. J. Transmembrane serine protease TADG-15 (ST14/Matriptase/MT-SP1): expression and prognostic value in ovarian cancer. *Br. J. Cancer*. **2005**, *92*, 278−283.
(18) Benaud, C. M.; Oberst, M.; Dickson, R. B.; Lin, C. Y. Deregulated activation of matriptase in breast cancer cells. *Clin. Exp. Metastasis* **2002**, *19*, 639−649.
(19) Suzuki, M.; Kobayashi, H.; Kanayama, N.; Saga, Y.; Suzuki, M.; Lin, C. Y.; Dickson, R. B.; Terao, T. Inhibition of tumor invasion by genomic down-regulation of matriptase through suppression of activation of receptor-bound pro-urokinase. *J. Biol. Chem.* **2004**, *279*, 14899−14908.
(20) Yamasaki, Y.; Satomi, S.; Murai, N.; Tsuzuki, S.; Fushiki, T. Inhibition of membrane-type serine protease 1/matriptase by natural and synthetic protease inhibitors. *J. Nutr. Sci. Vitaminol*. **2003**, *49*, 27−32.
(21) Parr, C.; Jiang, W. G. Hepatocyte growth factor activation inhibitors (HAI-1 and HAI-2) regulate HGF-induced invasion of human breast cancer cells. *Int. J. Cancer* **2006**, *119*, 1176−1183.
(22) Forbs, D.; Thiel, S.; Stella, M. C.; Sturzebecher, A.; Schweinitz, A.; Steinmetzer, T.; Sturzebecher, J.; Uhland, K. In vitro inhibition of matriptase prevents invasive growth of cell lines of prostate and colon carcinoma. *Int. J. Oncol.* **2005**, *27*, 1061−1070.

(23) Long, Y-Q.; Lee, S-L.; Lin, C-Y.; Enyedy, I. J.; Wang, S.; Li, P.; Dickson, B, R.; Roller, P. P. Synthesis and evaluation of the sunflower derived trypsin inhibitor as a potent inhibitor of the type II transmembrane serine protease, matriptase. *Bioorg. Med. Chem. Lett.* **2001**, *11*, 2515−2519.
(24) Korsinczky, M. L.; Schirra, H. J.; Rosengren, K. J.; West, J.; Condie, B. A.; Otvos, L.; Anderson, M. A.; Craik, D. J. Solution structures by 1H NMR of the novel cyclic trypsin inhibitor SFTI-1 from sunflower seeds and an acyclic permutant. *J. Mol. Biol.* **2001**, *311*, 579−591.
(25) Zablotna, E.; Kazmierczak, K.; Jaskiewicz, A.; Stawikowski, M.; Kupryszewski, G.; Rolka, K. Chemical synthesis and kinetic study of the smallest naturally occurring trypsin inhibitor SFTI-1 isolated from sunflower seeds and its analogues. *Biochem. Biophys. Res. Commun.* **2002**, *292*, 855−859.
(26) Descours, A.; Moehle, K.; Renard, A.; Robinson, J. A. A new family of beta-hairpin mimetics based on a trypsin inhibitor from sunflower seeds. *Chembiochem* **2002**, *3*, 318−323.
(27) Luckett, S.; Garcia, R. S.; Barker, J. J.; Konarev, A. V.; Shewry, P. R.; Clarke, A. R.; Brady, R. L. High-resolution structure of a potent, cyclic proteinase inhibitor from sunflower seeds. *J. Mol. Biol.* **1999**, *290*, 525−533.
(28) McBride, J. D.; Watson, E. M.; Brauer, A. B. E.; Jaulent, A. M.; Leatherbarrow, R. J. Peptide mimics of the Bowman-Birk inhibitor reactive site loop. *Biopolymers* **2002**, *66*, 79−92.
(29) Korsinczky, M. L. J.; Schirra, H. J.; Craik, D. J. Sunflower trypsin inhibitor-1. *Curr. Protein Pept. Sci.* **2004**, *5*, 351−364.
(30) Zablotna, E.; Kret, A.; Jaskiewicz, A.; Olma, A, Leplawy, M. T.; Rolka, K. Introduction of alpha-hydroxymethyamino acid residues in substrate specificity P1 position of trypsin inhibitor SFTI-1 from sunflower seeds retains its activity. *Biochem. Biophys. Res. Commun.* **2006**, *340*, 823−828.
(31) Hilpert, K.; Hansen, G.; Wessener, H.; Volkmer-Engert, R.; Höhne, W. Complete substitutional analysis of a sunflower trypsin inhibitor with different serine proteases. *J. Biochem (Tokyo)* **2005**, *138*, 383−390.
(32) Korsinczky, M. L. J.; Clark, R. J.; Craik, D. J. Disulfide bond mutagenesis and the structure and function of the head-to-tail macrocyclic trypsin inhibitor SFTI-1. *Biochemistry* **2005**, *44*, 1145−1153.
(33) Mulvenna, J. P.; Foley, F. M.; Craik, D. J. Discovery, structural determination, and putative processing of the precursor protein that produces the cyclic trypsin inhibitor sunflower trypsin inhibitor 1. *J. Biol. Chem.* **2005**, *280*, 32245−32253.
(34) Mosberg, H. I.; Omnaas, J. R. Dithioether-containing cyclic peptides. *J. Am. Chem. Soc.* **1985**, *107*, 2986−2987.
(35) Ueki, M.; Ikeo, T.; Iwadate, M.; Asakura, T.; Williamson, M. P.; Slaninova, J. Solid phase synthesis and biological activities of [Arg8]-vasopressin methylenedithioether. *Bioorg. Med. Chem. Lett.* **1999**, *9*, 1767−1772.
(36) Lindman, S.; Lindeberg, G.; Gogoll, A.; Nyberg, F.; Karlen, A.; Hallberg, A. Synthesis, receptor binding affinities and conformational properties of cyclic methylenedithioether analogues of angiotensin II. *Bioorg. Med. Chem.* **2001**, *9*, 763−772.
(37) McFadyen, I. J.; Ho, J. C.; Mosberg, H. I.; Traynor, J. R. Modifications of the cyclic mu receptor selective tetrapeptide Tyr-c[D-Cys-Phe-D-Pen]NH2 (Et): effects on opioid receptor binding and activation. *J. Pept. Res.* **2000**, *55*, 255−261.
(38) Szewczuk, Z.; Rebholz, K. L.; Rich, D. L. Synthesis and biological activity of new conformationally restricted analogues of pepstatin. *Int. J. Pept. Res.* **1992**, *40*, 233−242.
(39) (a) Kamenecka, T. M.; Danishefsky, S. J. Discovery through total synthesis: a retrospective on the himastatin problem. *Chem.-Eur. J.* **2001**, *7*, 41−63. (b) Kamenecka, T. M.; Danishefsky, S. J. Studies in the Total Synthesis of Himastatin: A revision of the stereochemical assignment. *Angew. Chem., Int. Ed.* **1998**, *37*, 2993−2995. (c) Kamenecka, T. M.; Danishefsky, S. J. Total synthesis of himastatin: confirmation of the revised stereostructure. *Angew. Chem., Int. Ed.* **1998**, *37*, 2995−2998. (d) Jou, G.; González, I.; Albericio, F.; Lloyd-Williams, P.; Giralt, E. Total synthesis of dehydrodidemnin B. Use of uronium and phosphonium salt coupling reagents in peptide synthesis in solution. *J. Org. Chem.* **1997**, *62*, 354−366.
(40) (a) Halpern, J. L. Antithrombotic therapy in atrial fibrillation: ximelagatran, an oral direct thrombin inhibitor. *Expert Rev. Cardiovasc. Ther.* **2004**, *2*, 163−174. (b) Serebruany, M. V.; Malinin, A. I.; Serebruany, V. L. Argatroban, a direct thrombin inhibitor for heparin-induced thrombocytopaenia: present and future perspectives. *Expert Opin. Pharmacother.* **2006**, *7*, 81−89.
(41) (a) Li, P.; Roller, P. P.; Xu, J. Current synthetic approaches to peptide and peptidomimetic cyclization. *Curr. Org. Chem.* **2002**, *6*, 411−440, and references cited therein. (b) Ueki, M.; Ikeo, T.; Nakamura, K.; Maruyama, T. Highly efficient solid phase cyclization of peptides by methylenedithioether or disulfide bond formation. In *Peptide Science* − Present and Future; Proceedings of the 1st International Peptide Symposium, December, Kyoto, Japan, 1997; Shimonishi, Y., Ed.; Springer: Dordrecht, The Netherlands, 2002; pp 539−541.

JM0704898